Thin Films

DOI: 10.1002/ange.201107867

Fabrication of Co-continuous Nanostructured and Porous Polymer Membranes: Spinodal Decomposition of Homopolymer and Random Copolymer Blends**

Le Li, Xiaobo Shen, Sung Woo Hong, Ryan C. Hayward, and Thomas P. Russell**

Multiphase polymeric materials with nanoscale structural co-continuity are of importance, for example, as active layers of organic photovoltaic cells, wherein donor and acceptor domains must interpenetrate on a scale commensurate with the diffusion length of excitons,[1] or as membranes for separation and fuel cells wherein continuous pathways for mass transport are required within a supporting matrix.[2] One route to such nanostructures is melt or solution state[3–5] self-assembly of block copolymers into bicontinuous morphologies. However, the requirements on the segmental interaction parameter and polymer composition are typically restrictive.[6] Bicontinuous microemulsions[7] also provide thermodynamically stable co-continuous structures of approximately 100 nm in size, but are similarly found over narrow ranges in phase space. Reactive blending can yield nanoscale co-continuity under some conditions, but typically requires suitably functionalized reactive precursor polymers.[8–10] An approach based on blending of polymer nanoparticles has been reported to give rise to nanoscale domains, but has not yet been shown to provide co-continuity.[11]

Spinodal phase separation of a polymer blend[12] presents an alternate route to co-continuous morphologies provided that the structure can be kinetically trapped at the desired length scale. The characteristic wavelength, ξ_0, of the initial spinodal structure is determined by a balance between diffusion and interfacial energy. For binary polymer blends, this is expressed in terms of the polymer chain size R_g and the interaction parameter χ:[13]

$$\xi_0 \approx R_g\left(\frac{\chi-\chi_s}{\chi_s}\right)^{-1/2}, \quad (1)$$

where χ_s is the value of χ at the spinodal temperature. The mixture reduces its energy by decreasing interfacial area, and thus the initial morphology (generally submicron size) evolves into increasingly large domains through self-similar coarsening of the co-continuous structure. As a result of the large molecular weights, M, of polymers, thermally induced demixing is feasible for a limited set of polymer pairs having a χ that is both small and significantly temperature dependent, for example, polystyrene/polyvinyl methyl ether[14,15] or polymethyl methacrylate/poly(styrene-*r*-acrylonitrile).[16,17] Because of the tendency for rapid structural coarsening, kinetic trapping of co-continuous morphologies has so far only been achieved on the micron scale.[18–20]

Solvent induced phase separation (SIPS),[21,22] that is, demixing driven by removal of a common solvent, is a more general method for immiscible polymer blends. Moreover, large quench depths can be achieved by rapid solvent evaporation, which according to Equation (1) may lead to the formation of nanoscale co-continuous structures. However, solvent also enhances mobility, thus increasing the rate of structural coarsening, and so SIPS typically yields large-scale structures (ca. 10 μm).[23–25] Additionally, since the solvent often has a preference for one component,[26] nucleation and growth (NG) is common for most compositions and quench depths. While spin-casting from almost nonselective solvents leads to spinodal decomposition (SD), the resulting kinetically trapped co-continuous structures are usually micron sized and therefore only two-dimensional in nature, and are found only over a narrow range of compositions[27] with nearly balanced substrate interactions.[28–31] In addition, even a slight difference in the component solubility gives rise to significant topography since the less soluble component solidifies first and eventually forms elevated domains.[29,32,33] While it has been argued that SIPS can yield phase-separated structures of tens of nanometers in size,[34–36] recent work has demonstrated that such morphologies result from crystallization rather than SD.[37–40]

Herein we demonstrate a SIPS approach for mixtures of homopolymers (A) with random copolymers (A-*r*-B) that yields smooth films with nanoscale co-continuous morphologies. The compositions of the random copolymers are chosen to tune the effective interaction parameter, χ_{eff}, thereby

[*] L. Li, X. Shen, S. W. Hong,[+] R. C. Hayward, T. P. Russell
Department of Polymer Science and Engineering
University of Massachusetts
Amherst, MA 01003 (USA)
E-mail: rhayward@mail.pse.umass.edu
russell@mail.pse.umass.edu
T. P. Russell
WPI-Advanced Institute for Materials Research (WPI-AIMR)
Tohoku University (Japan)
[+] Current address: Samsung Advanced Institute of Technology (SAIT), Gyeonggi-do (South Korea)

[**] Support for this work was provided by Polymer-Based Materials for Harvesting Solar Energy, an Energy Frontier Research Center funded by the U.S. Department of Energy, Office of Science, Office of Basic Energy (DE-SC0001087; support for L.L., R.C.H. and T.P.R.) and through contract (DE-FG02-96ER45612), and by World Premier International Research Center Initiative (WPI), MEXT, Japan. This work made use of facilitates supported by the NSF-MRSEC on Polymers at UMass (DMR-0820506).

Supporting information for this article is available on the WWW under http://dx.doi.org/10.1002/anie.201107867.

allowing the quench depth attained during solvent casting to be tailored, and trapping of the system by vitrification during the initial stages of SD. A simple spin-casting process yields co-continuous morphologies with characteristic sizes down to several tens of nanometers, and the method is not highly sensitive to the choice of solvent or substrate chemistry.

We design our polymer blend system based on the immiscible pair of polystyrene (PS) and poly(2-vinylpyridine) (P2VP), which exhibit a χ of approximately 0.2 at room temperature.[41,42] According to mean-field theory for random copolymer blends,[43–45] we expect that this interaction strength will be mediated by incorporating styrene monomers into the P2VP chains, that is, using P(S-*r*-2VP) random copolymers. While previous studies on homopolymer/random copolymer blends exist, their focus has been to test predicted phase behaviors and extract interaction parameters for immiscible homopolymer pairs.[33,44,46–52] For a binary A/A_x-*r*-B_{1-x} mixture, χ_{eff} should depend on x,[51,53] assuming equal segment volumes, according to:

$$\chi_{eff} = (1-x)^2 \chi_{AB}. \quad (2)$$

To achieve a modest degree of immiscibility, that is, $\chi_{eff}N \approx 5$–10, where N is the average degree of polymerization, we use a random copolymer P(S-*r*-2VP) with $M = 56\ kg\,mol^{-1}$ [denoted P(S-*r*-2VP)56k] and a mole fraction of styrene of $x = 0.70$, and blend it with PS homopolymers having $M = 26$, 34, and 55 $kg\,mol^{-1}$ (PS26k, PS34k, and PS55k, respectively; Table 1). Phase separation is induced by solvent evaporation during spin-casting of a 1:1 by weight mixture of PS and P(S-*r*-2VP) in toluene. Remarkably, as shown by the transmission electron microscope (TEM) images in Figure 1, the result is films with co-continuous structures having characteristic sizes as small as approximately 80 nm in the case of PS26k/P(S-*r*-2VP)56k (Figure 1a); such a size is unusual for macrophase separated polymer blends. Since this size scale is considerably less than the film thickness (ca. 500 nm), the co-continuous morphology is truly three-dimensional, rather than the two-dimensionally co-continuous micron-scale structures reported by others.[27,29–32] This is verified by cross-sectional TEM (Figure 1b), which confirms that the co-continuous morphology penetrates throughout the thickness, and reveals that the film has a smooth surface.

Table 1: Summary of polymers used in this study.

	Styrene [mol%]	M_w [$kg\,mol^{-1}$]	M_n [$kg\,mol^{-1}$]	PDI
P(S-*r*-2VP)39k	78	39	28	1.38
P(S-*r*-2VP)56k	70	56	40.5	1.38
PS26k	100	26	25	1.04
PS32k	100	32.4	30	1.08
PS34k	100	34	33	1.04
PS55k	100	55	54	1.02
PS136k	100	136	120	1.13
PS570k	100	570	520	1.10
P2VP38k	–	37.5	35	1.07

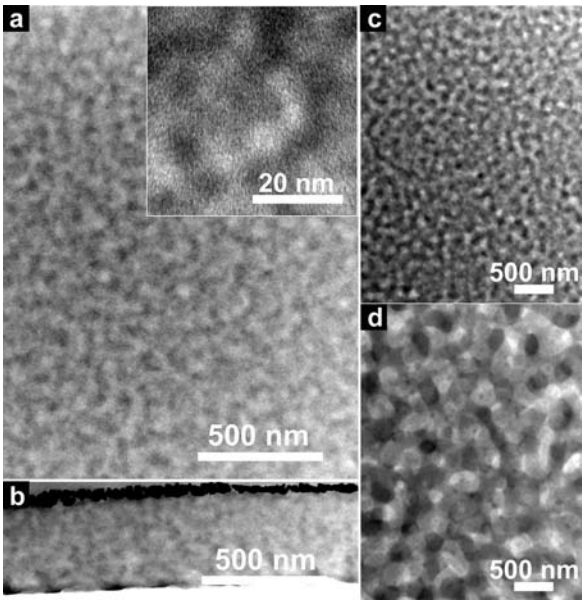

Figure 1. Plan-view TEM images of 1:1 (by weight) blends of PS/P(S-*r*-2VP)56k with PS having an M of 26k (a), 34k (c), and 55k (d). The images show co-continuous nanostructures with molecular-weight-dependent sizes. b) A cross-sectional TEM image of the same sample as shown in a) confirms that the co-continuous structure spans the film thickness. In all images, P(S-*r*-2VP)-rich phases appear darker because of staining with I_2 vapor.

During spin-casting, evaporation apparently quenches the system into the spinodal envelope so that demixing occurs by formation of a co-continuous morphology with a small characteristic wavelength. To reduce interfacial area, these domains coarsen over time, however, the speed of solvent removal is sufficiently fast to trap the structure because of vitrification at an early stage of coarsening. From Flory–Huggins theory, we estimate the critical χ to drive phase separation,

$$\chi_c = \frac{1}{2}\left(\frac{1}{\sqrt{N_1}} + \frac{1}{\sqrt{N_2}}\right)^2, \quad (3)$$

as approximately 6×10^{-3} for the PS26k/P(S-*r*-2VP)56k blend. Assuming that solvent at a volume fraction of ϕ_s serves only to dilute the unfavorable interactions between polymers,[54] phase separation should occur when $\chi_c = (1-\phi_s)\chi_{eff}$. From these considerations, we estimate that demixing occurs at $\phi_s \approx 70$ vol%. From the Fox equation and the glass transition temperatures (T_g) of the components (116 K for toluene[55] and ≈373 K for the polymers), we estimate that the T_g value of the mixture will reach room temperature at $\phi_s \approx 12$ vol%. Thus, the polymer solution is already fairly concentrated when demixing begins, and its viscosity will climb rapidly as solvent is evaporated and the glassy state is approached, thus allowing the kinetic trapping of nanoscale co-continuous structures.

The influence of molecular weight further supports this proposed mechanism. Increasing N should lead to phase separation at larger ϕ_s values, thus allowing for more extensive coarsening prior to vitrification, and thus providing

a means to tune length scale by adjusting the N value of either polymer. As expected, larger co-continuous structures were obtained for PS34k and PS55k (Figures 1b and c). Notably, the size scales observed, approximately 150 and 500 nm, respectively, depend more strongly on N than expected based on Equation (1). In fact, they are consistent with the amount of coarsening prior to vitrification setting the size scale obtained, rather than the initial length scale of demixing. Similar results were also found for a shorter random copolymer (39 kg mol^{-1}) having a lower 2VP content ($x = 0.78$; see the Supporting Information). Our findings demonstrate that understanding the interplay between thermodynamics (χ_{eff}) and kinetics (coarsening and vitrification) allows control over the morphologies formed by demixing.

To conclusively establish the co-continuity of these structures, we selectively extracted the P(S-*r*-2VP)-rich phase from blend films by immersion in methanol and acetic acid (1:1 by volume). As shown for a 1:1 (by weight) blend of PS55k/P(S-*r*-2VP)56k, plan-view TEM images on unstained samples showed excellent contrast (Figure 2a) after solvent extraction, as compared with Figure 1d where contrast could only be seen after I_2 staining. The porous nature of the film was revealed by scanning electron microscope (SEM), where open pores were present both on the film surface (Figure 2b) as well as percolating through the film thickness (Figure 2c), thereby establishing the continuity of the extracted domains. In contrast, for an asymmetric blend of 2:1 (by weight) PS55k/P(S-*r*-2VP)56k, P(S-*r*-2VP)-rich droplets dispersed in a PS-rich matrix were observed, characteristic of a morphology generated by NG. Solvent extraction followed by sample fracture led to pore formation only on the surface of the film, with the interior domains remaining intact (Figures 2d–f). Subsequent removal of random copolymer-rich domains from the cleaved films led to the appearance of discrete pores in the film cross-section (Figure 2g), thus confirming the presence of isolated droplets that are inaccessible to the selective solvent because of the surrounding PS-rich matrix.

We note that nanoporous membranes with continuous channels have been previously produced using block copolymer templates.[2,56–59] However, since these morphologies exist over narrow composition ranges, and each M gives rise to one specific size, stringently controlled polymerization conditions are required. Nanoporous metallic materials can be produced by the dealloying method,[60–64] however harsh conditions (i.e., high temperatures and corrosive acids) are employed. Given the simplicity of the SIPS process presented herein, and the access to a wide range of pore sizes from a simple set of homopolymers, it represents an attractive route for membrane fabrication.

To demonstrate the importance of using a random copolymer to reduce the χ_{eff} value, we also studied as-spun films for 1:1 (by weight) mixtures of PS26k and P2VP38k homopolymers. Since toluene is a non-solvent for P2VP, we instead used the nearly nonselective solvent chloroform. In contrast to the co-continuous morphologies seen for the PS/P(S-*r*-2VP) blends, the homopolymer system gave rise to larger (ca. 300–500 nm) P2VP-rich droplets within a PS-rich matrix (Figure 3a), thus suggesting that demixing has instead

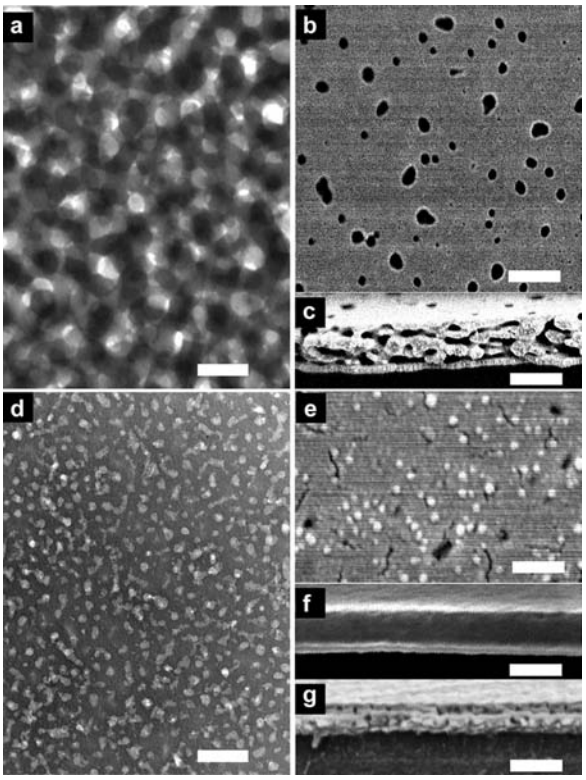

Figure 2. Thin membranes of blends of PS55k/P(S-*r*-2VP)56k after selective solvent extraction of the P(S-*r*-2VP)-rich phases. For a 1:1 (by weight) blend, the high degree of contrast from TEM on an unstained sample (a), coupled with SEM top-view images (b) showing pores at the free surface, and with cross-sectional images (c) showing pores percolating through the film thickness, indicate extraction of material from the co-continuous film. By contrast, for a 2:1 (by weight) blend, TEM (d) reveals only isolated domains of random copolymer-rich phases, while top-view (e) and cross-sectional (f) SEM images show that material has only been extracted from domains at the free surface. g) Cross-sectional SEM of the same sample in d–f), with exposure of the cross-section and selective extraction, shows discrete pores in the thin membrane (scale bars: 500 nm).

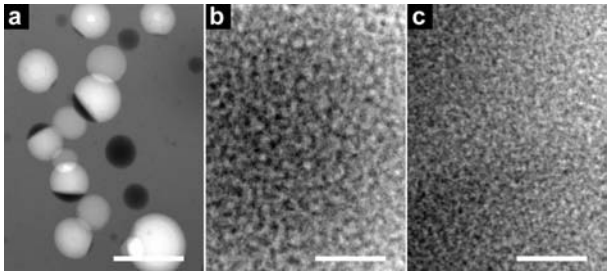

Figure 3. a) TEM image of a 1:1 (by weight) blend of PS26k/P2VP38k homopolymers spin-cast from chloroform showing droplets of P2VP-rich domains (dark circles) in a PS matrix. The white circles correspond to P2VP-rich domains that were extracted during floating of the film sample off of the substrate. TEM images of 1:1 (by weight) blends of PS26k/P(S-*r*-2VP)56k spin-cast from toluene (b) and chloroform (c) shown at the same magnification to highlight the dramatic difference in morphology obtained using the random copolymer blend. The P2VP-rich phases appear darker because of staining with I_2 vapor (scale bars: 500 nm).

occurred by NG. To ensure that the choice of solvent was not responsible for this dramatic difference, we also spin-cast a PS26k/P(S-*r*-2VP)56k blend film from chloroform (Figure 3c; see Figure S2 in the Supporting Information for further details), which gave a co-continuous morphology similar to that from toluene (Figure 3b).

Given the three-dimensional nature of these co-continuous structures we expect less dependence of the morphology on the substrate than in previous reports.[29,31,32] To this end, we tested four substrates including silicon wafers with a native oxide layer, gold-coated silicon, mica, and polyimide films. In all cases similar co-continuous morphologies were observed (Figure 4) with a thin wetting layer of the PS-rich phase at the

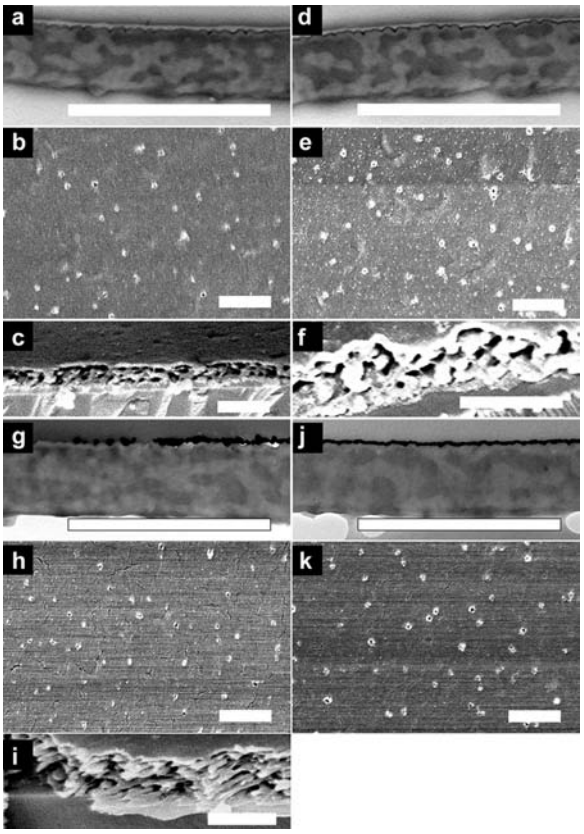

Figure 4. Blend films of 1:1 (by weight) PS26k/P(S-*r*-2VP)56k prepared on a silicon wafer (a–c), a gold-coated silicon wafer (d–f), a mica substrate (g–i), and a polyimide substrate (j–k). Cross-sectional TEM images (a, d, g and j), and top-view (b, e, h and k) and cross-sectional (c, f and i) SEM images after selective solvent extraction of P(S-*r*-2VP)-rich domains. Similar co-continuous structures are observed, regardless of the substrate type (scale bars: 1 μm).

free surface resulting from the lower surface energy of PS. For the case of silicon and gold substrates, preferential wetting by P(S-*r*-2VP) results in a random copolymer-rich layer at the polymer/substrate interface (Figure 4a and d), while little preference was found in the case of mica and Kapton (Figures 4g and j).

Based on the idea that slower evaporation should yield more extensive coarsening, we also varied the conditions of film casting. For spin-cast films, the size of co-continuous structures was found to vary nearly linearly with film thickness (see Figure S3 in the Supporting Information). For significantly thicker (ca. 10 μm) films by drop casting, co-continuous structures were retained, but with a significant gradient in size through the thickness (Figure 5). Near the polymer/air interface, the characteristic length scale was

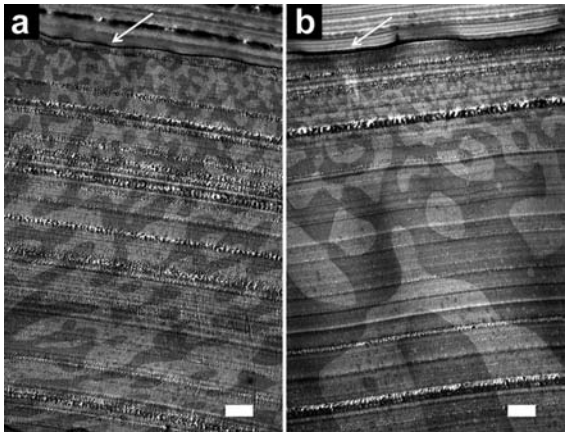

Figure 5. Cross-sectional TEM micrographs of thick membranes of 1:1 (by weight) blends of PS32k/P(S-*r*-2VP)56k. a) The co-continuous structures formed upon drop-casting show a gradient in the length scale of the co-continuous structure through the film thickness. b) After annealing with the substrate held at 120°C for 10 min while the free surface was cooled, the gradient is enhanced (scale bars: 1 μm). P(S-*r*-2VP) phases appear darker because of staining with I_2 vapor; the dark lines (indicated by arrows) represent gold films deposited to mark the polymer/air interface.

approximately 500 nm, while at the bottom surface it was approximately 2 μm. In these thick films, evaporation yields a gradient in solvent concentration, causing the surface of the film to vitrify while the remainder has sufficient solvent to allow coarsening. This gradient can be further enhanced by annealing, that is, by applying heat to the substrate while blowing cold nitrogen gas onto the surface of the film (Figure 5b). Such gradient structures with continuous channels are of potential interest for applications as filtration membranes,[65] although we note that significant development would be necessary before this approach could compete with the current phase inversion method to fabricate filtration membranes.

Finally, we consider the alternative explanation that the co-continuous morphologies in PS/P(S-*r*-2VP) blends is due to microphase separation of the random copolymer, with PS homopolymer swelling the PS-rich microdomains.[66,67] Small angle X-ray scattering (SAXS) on P(S-*r*-2VP) samples (see Figures S4a and S4b in the Supporting Information) shows a monotonic decay in intensity. Fitting the SAXS data using the Debye–Bueche equation results in a correlation length a of 3.5 nm for both P(S-*r*-2VP)s (Figure S4c).[38] The chord lengths for a two-phase system can be extracted from $l_i = a/\phi_j$, where ϕ_i is the volume fraction of phase i, were found to be 16 nm for PS-rich domains and 4.5 nm for P(S-*r*-2VP)-rich domains in P(S-*r*-2VP)39k, and 12 nm and 5 nm in P(S-*r*-2VP)56k. TEM micrographs (Figures S4d and S4e) of I_2-

stained P(S-*r*-2VP)s exhibit similar contrast as the I_2-stained PS homopolymer sample (Figure S4f), with a feature size of several nanometers. The observed length scales of 50 nm to 300 nm for the blend systems, as well as their coarsening upon thermal annealing strongly suggest that microphase separation is not responsible for the observed behavior. Consequently, we conclude that the co-continuous morphologies formed here result from kinetically-trapped demixing of PS and P(S-*r*-2VP), rather than microphase separation.

In summary, we have developed a strategy to tune incompatibility in immiscible polymer blends through the use of a random copolymer, thus allowing quenches into the spinodal envelope during solvent casting followed closely by vitrification. This simple method yields co-continuous morphologies with sizes down to tens of nanometers, and is robust to variations in solvent choice and substrate chemistry, and provides simple means to control the sizes of the structures obtained. These co-continuous films further serve as templates for thin nanoporous membranes and thick membranes with gradients in feature size, thus offering potential promise in applications such as filtration membranes.

Received: November 8, 2011
Revised: January 12, 2012
Published online: March 16, 2012

Keywords: amorphous materials · electron microscopy · nanostructures · polymers · thin films

[1] H. Hoppe, N. S. Sariciftci, *J. Mater. Chem.* **2006**, *16*, 45.
[2] M. Ulbricht, *Polymer* **2006**, *47*, 2217.
[3] A. Dehsorkhi, V. Castelletto, I. W. Hamley, P. J. F. Harris, *Soft Matter* **2011**, *7*, 10116.
[4] B. E. McKenzie, F. Nudelman, P. H. H. Bomans, S. J. Holder, N. Sommerdijk, *J. Am. Chem. Soc.* **2010**, *132*, 10256.
[5] K. Hales, Z. Y. Chen, K. L. Wooley, D. J. Pochan, *Nano Lett.* **2008**, *8*, 2023.
[6] F. S. Bates, G. H. Fredrickson, *Annu. Rev. Phys. Chem.* **1990**, *41*, 525.
[7] F. S. Bates, W. W. Maurer, P. M. Lipic, M. A. Hillmyer, K. Almdal, K. Mortensen, G. H. Fredrickson, T. P. Lodge, *Phys. Rev. Lett.* **1997**, *79*, 849.
[8] H. Pernot, M. Baumert, F. Court, L. Leibler, *Nat. Mater.* **2002**, *1*, 54.
[9] S. Ishino, H. Nakanishi, T. Norisuye, Q. Tran-Cong-Miyata, Y. Awatsuji, *Macromol. Rapid Commun.* **2006**, *27*, 758.
[10] B. S. Kim, T. Chiba, T. Inoue, *Polymer* **1995**, *36*, 43.
[11] T. Kietzke, D. Neher, K. Landfester, R. Montenegro, R. Guntner, U. Scherf, *Nat. Mater.* **2003**, *2*, 408.
[12] J. W. Cahn, *Acta Metall.* **1961**, *9*, 795.
[13] J. J. Van Aartsen, *Eur. Polym. J.* **1970**, *6*, 919.
[14] T. K. Kwei, T. Nishi, R. F. Roberts, *Macromolecules* **1974**, *7*, 667.
[15] M. Bank, J. Leffingw, C. Thies, *Macromolecules* **1971**, *4*, 43.
[16] K. Naito, G. E. Johnson, D. L. Allara, T. K. Kwei, *Macromolecules* **1978**, *11*, 1260.
[17] W. A. Kruse, R. G. Kirste, J. Haas, B. J. Schmitt, D. J. Stein, *Macromol. Chem. Phys.* **1976**, *177*, 1145.
[18] H. Chung, K. Ohno, T. Fukuda, R. J. Composto, *Nano Lett.* **2005**, *5*, 1878.
[19] L. Li, C. Miesch, P. K. Sudeep, A. C. Balazs, T. Emrick, T. P. Russell, R. C. Hayward, *Nano Lett.* **2011**, *11*, 1997.
[20] H. Tanaka, A. J. Lovinger, D. D. Davis, *Phys. Rev. Lett.* **1994**, *72*, 2581.
[21] K. Solc, Y. C. Yang, *Macromolecules* **1988**, *21*, 829.
[22] J. S. Gutmann, P. Müller-Buschbaum, M. Stamm, *Faraday Discuss.* **1999**, *112*, 285.
[23] J. H. Aubert, R. L. Clough, *Polymer* **1985**, *26*, 2047.
[24] I. Hopkinson, M. Myatt, *Macromolecules* **2002**, *35*, 5153.
[25] A. T. Young, *J. Vac. Sci. Technol. A* **1986**, *4*, 1128.
[26] C. C. Hsu, J. M. Prausnitz, *Macromolecules* **1974**, *7*, 320.
[27] K. Dalnoki-Veress, J. A. Forrest, J. R. Stevens, J. R. Dutcher, *Physica A* **1997**, *239*, 87.
[28] G. Krausch, E. J. Kramer, M. H. Rafailovich, J. Sokolov, *Appl. Phys. Lett.* **1994**, *64*, 2655.
[29] S. Walheim, M. Boltau, J. Mlynek, G. Krausch, U. Steiner, *Macromolecules* **1997**, *30*, 4995.
[30] K. Dalnoki-Veress, J. A. Forrest, J. R. Stevens, J. R. Dutcher, *J. Polym. Sci. Part B* **1996**, *34*, 3017.
[31] G. Krausch, *Mater. Sci. Eng. R* **1995**, *14*, 1.
[32] M. Boltau, S. Walheim, J. Mlynek, G. Krausch, U. Steiner, *Nature* **1998**, *391*, 877.
[33] S. Affrossman, G. Henn, S. A. Oneill, R. A. Pethrick, M. Stamm, *Macromolecules* **1996**, *29*, 5010.
[34] S. E. Shaheen, C. J. Brabec, N. S. Sariciftci, F. Padinger, T. Fromherz, J. C. Hummelen, *Appl. Phys. Lett.* **2001**, *78*, 841.
[35] A. C. Arias, J. D. MacKenzie, R. Stevenson, J. J. M. Halls, M. Inbasekaran, E. P. Woo, D. Richards, R. H. Friend, *Macromolecules* **2001**, *34*, 6005.
[36] C. Y. Yang, A. J. Heeger, *Synth. Met.* **1996**, *83*, 85.
[37] D. Chen, F. Liu, C. Wang, A. Nakahara, T. P. Russell, *Nano Lett.* **2011**, *11*, 2071.
[38] D. A. Chen, A. Nakahara, D. G. Wei, D. Nordlund, T. P. Russell, *Nano Lett.* **2011**, *11*, 561.
[39] N. D. Treat, M. A. Brady, G. Smith, M. F. Toney, E. J. Kramer, C. J. Hawker, M. L. Chabinyc, *Adv. Energy Mater.* **2011**, *1*, 82.
[40] M. Campoy-Quiles, T. Ferenczi, T. Agostinelli, P. G. Etchegoin, Y. Kim, T. D. Anthopoulos, P. N. Stavrinou, D. D. C. Bradley, J. Nelson, *Nat. Mater.* **2008**, *7*, 158.
[41] K. H. Dai, E. J. Kramer, *Polymer* **1994**, *35*, 157.
[42] M. F. Schulz, A. K. Khandpur, F. S. Bates, K. Almdal, K. Mortensen, D. A. Hajduk, S. M. Gruner, *Macromolecules* **1996**, *29*, 2857.
[43] D. R. Paul, J. W. Barlow, *Polymer* **1984**, *25*, 487.
[44] R. P. Kambour, J. T. Bendler, R. C. Bopp, *Macromolecules* **1983**, *16*, 753.
[45] G. ten Brinke, F. E. Karasz, W. J. Macknight, *Macromolecules* **1983**, *16*, 1827.
[46] F. Bruder, R. Brenn, *Macromolecules* **1991**, *24*, 5552.
[47] R. P. Kambour, J. T. Bendler, *Macromolecules* **1986**, *19*, 2679.
[48] G. R. Strobl, J. T. Bendler, R. P. Kambour, A. R. Shultz, *Macromolecules* **1986**, *19*, 2683.
[49] R. P. Kambour, J. T. Bendler, *Macromolecules* **1986**, *19*, 2679.
[50] R. Vukovic, G. Bogdanic, F. E. Karasz, W. J. MacKnight, *J. Phys. Chem. Ref. Data* **1999**, *28*, 851.
[51] G. Alberda van Ekenstein, R. Meyboom, G. ten Brinke, O. Ikkala, *Macromolecules* **2000**, *33*, 3752.
[52] P. S. Alexandrovich, Univerisity of Massachusetts (Amherst), **1978**.
[53] R. L. Scott, *J. Polym. Sci.* **1952**, *9*, 423.
[54] R. L. Scott, *J. Chem. Phys.* **1949**, *17*, 279.
[55] A. Kudlik, C. Tschirwitz, S. Benkhof, T. Blochowicz, E. Rossler, *Europhys. Lett.* **1997**, *40*, 649.
[56] H. Uehara, T. Yoshida, M. Kakiage, T. Yamanobe, T. Komoto, K. Nomura, K. Nakajima, M. Matsuda, *Macromolecules* **2006**, *39*, 3971.
[57] L. M. Pitet, M. A. Amendt, M. A. Hillmyer, *J. Am. Chem. Soc.* **2010**, *132*, 8230.
[58] B. H. Jones, T. P. Lodge, *J. Am. Chem. Soc.* **2009**, *131*, 1676.

[59] M. A. Hillmyer, in *Block Copolymers II*, *Vol. 190* (Ed.: V. Abetz), Springer, Berlin, **2005**, p. 137.
[60] M. Raney, US Patent 1628190, **1927**.
[61] S. G. Corcoran, G. S. Chakarova, K. Sieradzki, *J. Electroanal. Chem.* **1994**, *377*, 85.
[62] D. V. Pugh, A. Dursun, S. G. Corcoran, *J. Mater. Res.* **2003**, *18*, 216.
[63] Y. Waku, N. Nakagawa, T. Wakamoto, H. Ohtsubo, K. Shimizu, Y. Kohtoku, *Nature* **1997**, *389*, 49.
[64] Y. Suzuki, P. E. D. Morgan, T. Ohji, *J. Am. Ceram. Soc.* **2000**, *83*, 2091.
[65] R. E. Kesting, *Synthetic polymeric membranes: a structural perspective*, Wiley-Interscience, New York, **1985**.
[66] H. Tanaka, H. Hasegawa, T. Hashimoto, *Macromolecules* **1991**, *24*, 240.
[67] M. W. Matsen, *Macromolecules* **1995**, *28*, 5765.

